Computational searching and mutagenesis suggest a structure for the pentameric transmembrane domain of phospholamban

Paul D. Adams[1], Isaiah T. Arkin[1,2], Donald M. Engelman[1] and Axel T. Brünger[3]

Structural and environmental constraints greatly simplify the folding problem for membrane proteins. Computational methods can be used in a global search to find a small number of chemically reasonable models within these constraints, such that a modest set of experimental data can distinguish among them. We show that, for phospholamban, the global search can be further simplified by reducing the problem to two-body, rather than many-body, interactions. This method of a constrained global search combined with experimental mutagenesis data yields a three-dimensional structure for this pentameric ion channel. The model is a left-handed symmetric homopentamer of α-helices with a well-defined channel, lined solely by hydrophobic residues.

[1]Department of Molecular Biophysics and Biochemistry, Yale University, New Haven, Connecticut 06520, USA
[2]Department of Cell Biology, Yale University, New Haven, Connecticut 06520, USA
[3]The Howard Hughes Medical Institute and Department of Molecular Biophysics and Biochemistry, Yale University, New Haven, Connecticut 06520, USA

The contraction/relaxation cycle of muscle is regulated by cytosolic levels of Ca^{2+} ions. For cardiac muscle cells to relax after contraction a rapid transfer of Ca^{2+} from the cytosol into the sarcoplasmic reticulum (SR) lumen is required. This transfer is achieved by the Ca^{2+}-ATPase of the SR. It has been shown that this pump is activated by cyclic AMP- and calmodulin-dependent phosphorylation of phospholamban (PLN), an integral membrane protein of the SR[1]. Cross-linking experiments suggest that phosphorylation of PLN promotes dissociation of an inhibitory complex formed between PLN and the Ca^{2+}-ATPase, activating the latter[2]. The putative transmembrane (TM) domain of PLN is predominantly α-helical[3] and forms a homopentamer[4]. PLN has also been shown to have ion-channel properties of its own in reconstituted lipid membranes[4]. Electrophysiological experiments demonstrate that PLN has a high specificity for Ca^{2+} ions and that inhibition of ion-channel activity can be produced with Cd^{2+} ions[4,5]. It is possible that the ion-channel activity of PLN is also important in its function as a regulator of the Ca^{2+}-ATPase.

The creation and breakdown of electrochemical gradients across membranes is important for energy transduction and the regulation of numerous cellular processes. There is a wealth of experimental data available for many of the membrane proteins involved; however, structural information has not been forthcoming. In part, this is due to the large size of many of these proteins, but also because of their transmembrane environment. Although structural information is available for certain ion-channel forming, non-DNA-encoded, fungal peptides such as gramicidin and alamethicin[6–8], they contain amino acids with unique structural properties making direct comparison with DNA-encoded ion channels difficult. Limited structural information has recently been obtained for the nicotinic acetylcholine receptor using electron diffraction[9]. The five central α-helices, which are thought to line the pore of this channel, could be observed but other transmembrane structural features were less easy to define. PLN has a passive ion-channel activity (it forms a pore through the membrane bilayer) but, in contrast to other DNA-encoded ion-channel forming proteins, it is very small (52 amino acids for the monomer). PLN, therefore, provides a simple system for the study of passive ion-channel structure. Here we present the construction of a molecular model for PLN using a global conformational search by computational methods combined with a mutagenesis analysis based on oligomerization[10–12].

Restrained modelling

There are many integral membrane proteins whose functions depend on the successful formation of oligomers through interactions between transmembrane α-helices[13]. High-resolution structural information about such integral membrane proteins has proved difficult to obtain using conventional structure determination techniques (crystallography or solution nuclear magnetic resonance). A combination of qualitative experimental observations and computational methods can be used to determine the most probable structures[10,11]. The number of experimental observations may be very small but limiting constraints can be included based on the amino acid sequence, ideal chemical parameters, secondary

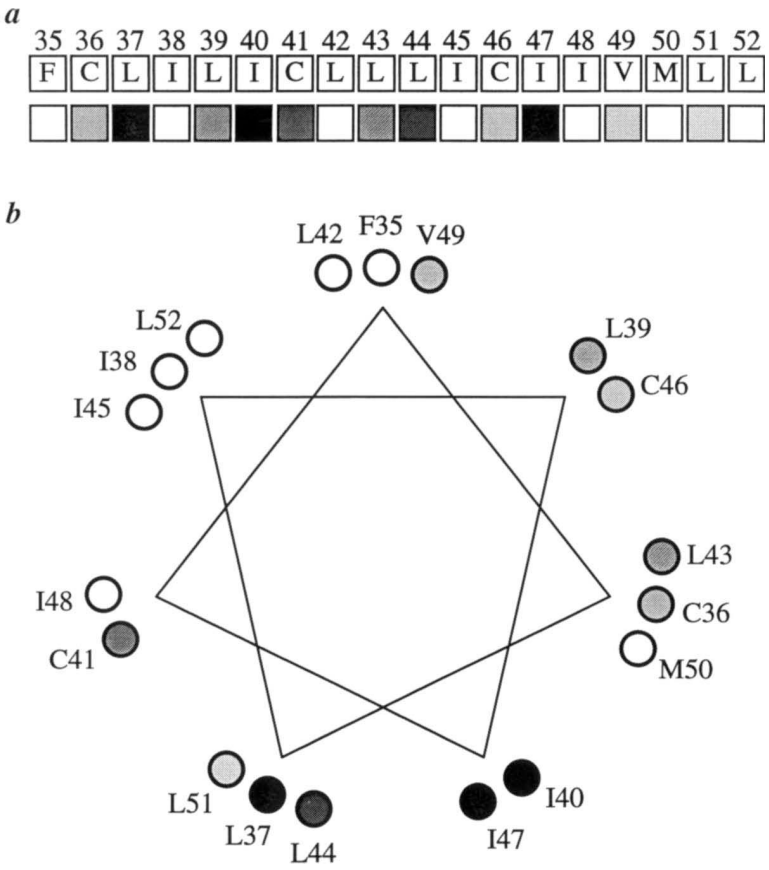

Fig. 1 *a*, Results of mutational sensitivity analysis (the mutational index P_i) for residues in the transmembrane region of PLN. A greyscale is used, with black indicating high sensitivity to mutation, decreasing through shades of grey to white indicating insensitivity to mutation. *b*, The results of mutational sensitivity analysis for residues in the transmembrane region of PLN shown on a helical wheel with a pitch of 3.5 residues per turn (that is geometrically consistent with a left-handed coiled-coil).

structure and the environment. Molecular modelling can be carried out by an extensive and systematic conformational search. Prior knowledge and some conservative assumptions can be used to limit the scope of the search to relevant regions of conformation space.

The existence of highly specific interactions between transmembrane helices has been demonstrated using mutational sensitivity analysis[14]. Several types of interactions are involved in driving the association of these helices: polar interactions (electrostatic), packing (van der Waals'), interactions between protein and lipid, and also between protein and solvent. The two stage model for the folding of polytopic α-helical membrane proteins proposes that individually-stable transmembrane helices interact with one another to form the folded conformation without changes in secondary structure[15]. If this is so, conformational searches can be simplified by maximizing the interaction (or complementarity) between the independently folded secondary structure elements. While the energy of the system alone may not be a reliable indicator of model correctness[16], the careful consideration of mutagenesis data allows a critical, independent test of any proposed model.

The complexes formed by many helical transmembrane proteins consist of more than two subunits and in many cases they are heteromeric. Complete search methods that sample all possible helix–helix interactions for such systems[10,17,18] would be very time consuming if not impossible. The computational cost of a complete heteromeric search without assuming symmetry rises with the power of the number of helices. If, however, a complex helical membrane protein can be sucessfully modelled as a set of pairwise helix interactions, the problem is approachable, as the computational cost is only of order two. We have conducted a pairwise search to generate a structure for the PLN pentamer and compared it with the result of a fivefold symmetric search. Both methods converged to the same structure, which could be selected from the small set of possible structures on the basis of a satisfactory match to mutagenesis data.

Mutagenesis studies of PLN pentamerization[12] have concentrated on the last 18 amino acids of the human PLN sequence (FCLILICLLLICIIVMLL, residues 35–52; Fig.1*a*, *b*), which are likely to comprise the transmembrane region of PLN based on their hydrophobicity. The α-helical nature of a truncated PLN sequence (residues 25–52) has been shown by both circular-dichroism[3] and Fourier transform infrared spectroscopy (I.T.A. *et al.*, manuscript in preparation). The putative TM helices of PLN are expected to be parallel in direction, based on their insertion into the bilayer through a common pathway. We assume that the helices are in contact throughout their length. These observations and assumptions were implemented during the conformational searches by using backbone hydrogen-bond and helix-axis restraints. In all calculations the 18 residue sequence studied by mutagenesis was simulated.

Exhaustive two-body search

The conformations of pairs of PLN transmembrane helices were searched with rotation angles α and β of 0°–360° for helices A and B respectively(Fig. 2*a*), starting with both left- and right-handed crossing angles, Ω. The sampling step size was 45° (extensive tests indicated this was an optimum value which maintained unbiased sampling of rotation space yet minimized the computational cost of the search), and four trials were carried out starting from each conformation using simulated annealing of all atomic coordinates leaving rotation- and crossing-angles free to vary. The resulting structures were analyzed to determine the final crossing angle (that is left-handed or right-handed) and rotation angles of both helices (Fig. 2*b*). In addition, the interaction energy between helices, the geometric helical parameters and the frequency of structures appearing in a particular region of interaction space were calculated (Fig. 2*c*). Two-body interactions were identified which are most consistent with a pentameric arrangement of helices, that is a relationship between α and β which when propagated to five helices produces a symmetric pentamer (Fig. 2*b*). The results indicate twelve sufficiently populated regions approximately consistent with a pentameric interaction. It should be noted that ten of these regions are left-

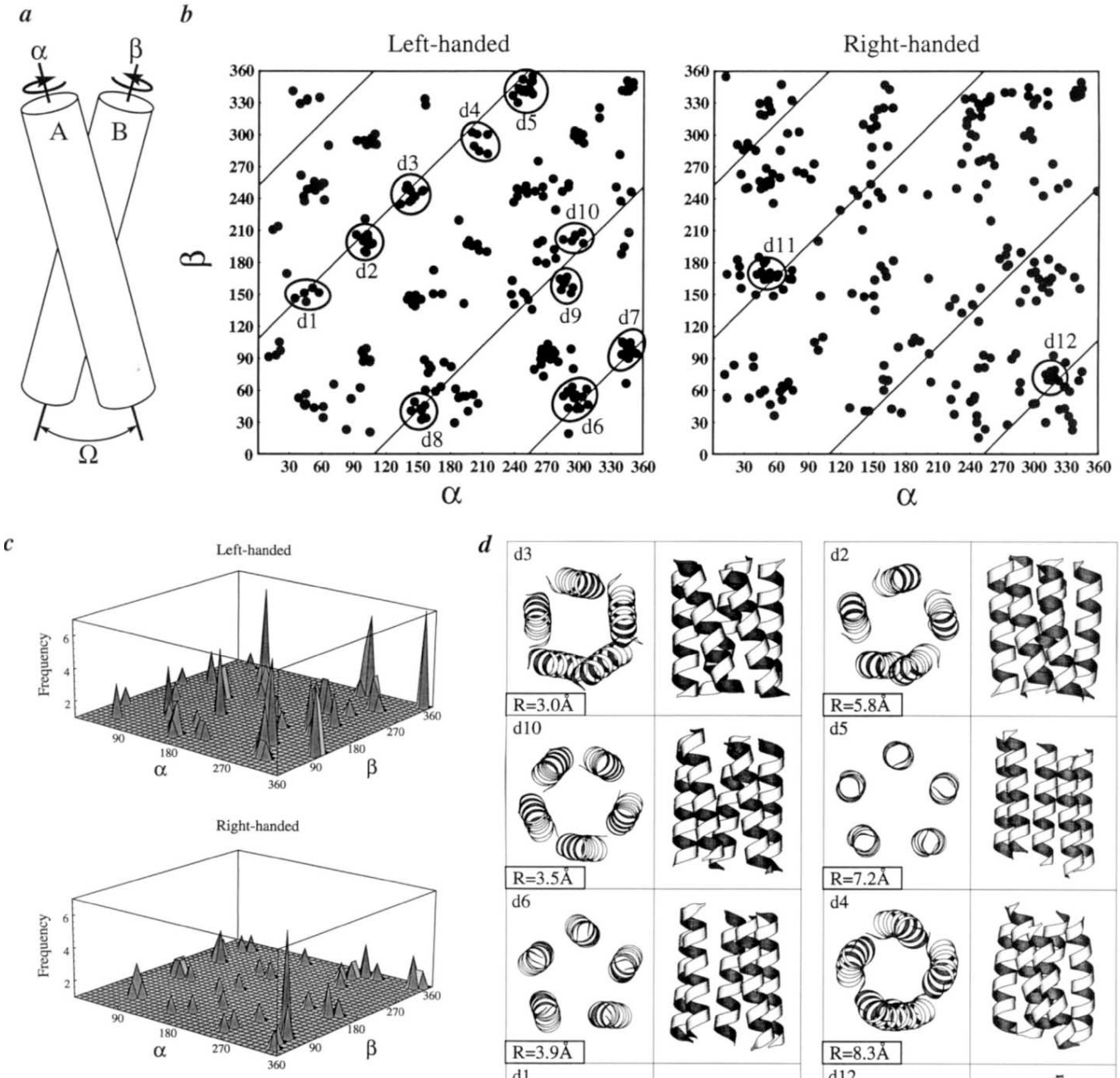

Fig. 2 *a*, The helix rotation parameters α and β were systematically varied in the two-body search. *b*, Frequency of structures obtained by simulated annealing found in α/β rotation space, averaged over a 10° by 10° grid, for left-handed and right-handed helical pairs. Lines indicate the regions with a pentameric relationship between α and β. The twelve clusters which were consistent with a pentameric interaction are marked (d1–d12). These clusters were used to generate single averaged structures and then refined. *c*, Distribution of final α, β rotation angles for all structures obtained by simulated annealing with a final left-handed or right-handed crossing angle. *d*, Pentamers generated from ten of the refined average structures. The models are ranked from top to bottom and left to right by their pentameric residual (*R*, equation 1). Models d8 and d9 are excluded because they did not form closed structures (*R*=43.7 and *R*=34.1 respectively).

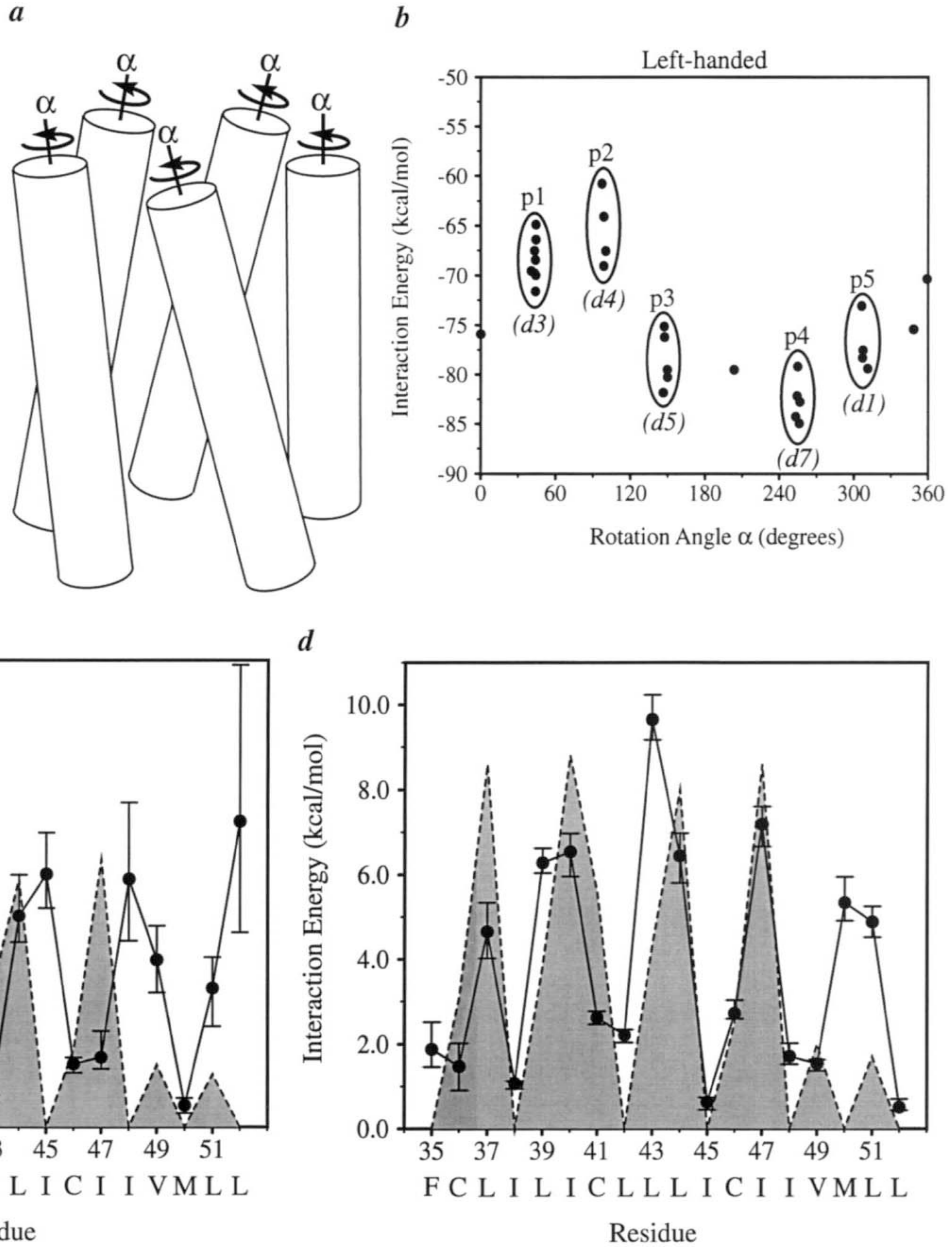

Fig. 3 *a*, The helix rotation parameter α was systematically varied for all helices simultaneously in the symmetric pentamer search. *b*, Interaction energy against rotation angle α for left-handed pentamers. The five clusters marked (p1-p5) were used to generate single averaged structures. The lower identifiers (italics) indicate the corresponding dimer models (Fig. 2*c*). *c* and *d*, Average interaction energy per residue (solid line) compared to the sensitivity of each residue to mutation (dashed line) for the lowest energy model (*c*) p4 and (*d*) p1. Error bars indicate the minimum and maximum value within the pentamer model.

handed while only two are right-handed. This bias towards left-handed structures is consistent with the mutation data, which best fit α-helices in a left-handed coiled-coil conformation (Fig. 1*b*). Average, refined models were generated from these clusters.

Helical pairs to pentamers

After refinement of the twelve models, pentamers were generated from the average models of pairs of helices by repeated application of the rotational and translation relationships between the two helices (Fig. 2*d*). It can be seen by visual inspection that many of the structures generated are approximately pentameric, the most obvious exception being the right-handed models (d11 and d12) which are much closer to tetramers. The pentameric residual R (equation 1) indicates that model d3 best forms a pentamer. Model d3 also shows the best correlation with the mutational data (Fig. 4*a*), with sensitive residues lying on the internal face of the pentamer and non-sensitive residues lying on the external face. This pentamer model was therefore further refined by use of simulated annealing and energy minimization.

Symmetric pentamer search

A systematic search starting from symmetric pentamers was carried out independent of the two-body search, with both left-handed and right-handed initial conformations (Fig. 3*a*). The helix conformations were searched with the helix rotation angle α between 0° and 360°. Structures were analysed after the simulated annealing proto-

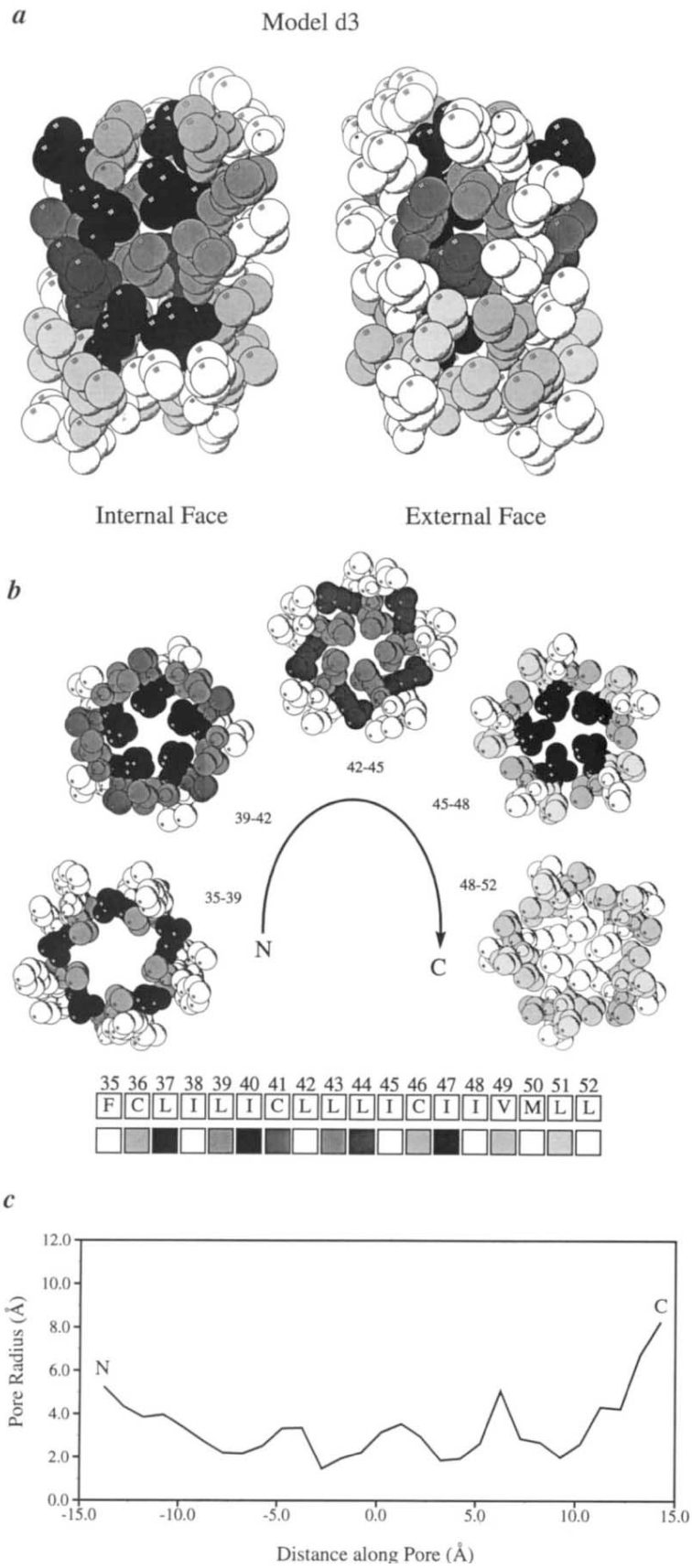

col. The root-mean-square fit to a cylinder was used to determine which pentamers were still approximately symmetric after annealing, ($P_{r.m.s.d.}$ < 1.5 Å). A plot of the helix rotation angle against average interaction energy for left-handed pentamers shows five well defined energy minima (Fig. 3*b*). There were very few symmetric pentameric right-handed structures found after simulated annealing (data not shown): selection of right-handed pentamers using $P_{r.m.s.d.}$ < 1.5 Å did not retrieve any models, and even when the selection criterion was relaxed ($P_{r.m.s.d.}$ < 2.0 Å) only six structures were found, defining two poorly populated energy minima.

This result strongly suggests that the PLN transmembrane sequence is unable to form a stable right-handed pentameric structure. Average structures were calculated for the five left-handed energy minima found. There is a well defined energy minimum at approximately $\alpha = 250°$ (model p4; Fig. 3*b*). A comparison between the interaction energy per residue and the experimental mutational sensitivity shows a strong anti-correlation for model p4 (Fig. 3*c*). It is assumed that sensitivity to mutation indicates residues which contribute to stability through packing interactions. Of the five most stable pentameric structures only one model shows a strong correlation with the mutation data, model p1 (Fig. 3*d*). It is interesting to note that the ensemble of structures used to generate this model were the most pentameric in character ($P_{r.m.s.d.}$ < 0.9 Å) and that this is also the most populated energy minimum found in the search.

The phospholamban model

The final phospholamban model is a left-handed pentamer which shows a high level of symmetry. The crossing angle (Ω) between adjacent helices is 16.7°, the separation between neighbouring helices is 10 Å and the average number of residues per turn for each helix is approximately 3.64. These geometric parameters are consistent with a left-handed coiled-coil interaction between the helices and are also similar to results obtained in another, unrelated helix bundle modelling study[19].

Two-body *vs* pentamer search

One of our goals in this study was to use the information from two-helix searches to model higher order oligomers. If this simplification succeeds, it could lead to a greatly enhanced computational approach to the study of membrane protein structure. The models produced from the independent two-body and pentamer searches (d3 and p1 respectively) are very similar to one another, with 0.6 Å r.m.s. deviation for Cα atoms, 1.63 Å r.m.s.

Fig. 4 Space-filling representations of the best models from the two-body and pentamer searches. In both cases residues have been shaded according to their experimentally determined sensitivity to mutation (Fig. 1). *a*, Model d3 (best two-helix model), internal and external face. *b*, Model p1 (best pentamer model), shown as sections through the pentamer (along the pentamer axis). The residues in each section are indicated, their identity and average sensitivity to mutation are shown in the lower scale. *c*, Pore radius for model p1 as a function of the distance travelled along the pore (from N to C terminus).

deviation for all atoms (and almost identical geometric parameters). Therefore, it would have been possible to generate the pentameric structure purely on the basis of the two-body search alone, in combination with the mutagenesis sensitivity data[12]. In the case of a symmetric homopentamer such as PLN the computational cost for a two-body search and symmetric pentamer search are approximately equivalent. When considering asymmetric hetero-oligomers, however, the computational cost of several two-body searches will be much less than one complete oligomer search. Although time consuming, such systematic searches are within the scope of current high performance parallel computing technology. The results presented here suggest that information from two-body searches alone may be sufficient to determine the correct conformation of an oligomer of helices.

Although the correlation between the mutational index and the interaction energy is high (Fig. 3*d*) for the best model, there are still some discrepancies, in particular residue 43 and the four caroboxy-terminal residues. In the case of Leu 43, these may be due to difficulties in distinguishing partial disruption from wild-type in the mutagenesis results. In the case of the four C-terminal residues the lack of a molecular environment in the simulations may distort their contribution to the stability of the model. Explicit inclusion of the lipid and water environment, although desirable, is not currently possible because of the extensive computing time required and inadequacies in force field parameters. Since all simulations were carried out *in vacuo* and distance restraints between helices were imposed, a compact structure with maximized packing interactions was obtained. If the four C-terminal amino acids are replaced with alanines, our simulations show that the symmetric pentamer search reveals a single preferred structure identical with our proposed model.

Prediction of tertiary structure at the atomic level based purely on sequence information is a challenging goal. A particular problem is still the selection of the correct model from a group of several candidates. Our work shows that, while it is possible to limit the number of models using an extensive search method, no simple criteria were capable of determining which model is most appropriate; in fact, the use of the lowest energy as a criterion selects an incorrect model (Fig. 3*b*, *c*). At the present state of computational methodology it appears that verification through direct experimental observations is essential. The contribution of a global computational search is to direct attention to a small number of chemically reasonable models. The information gained through mutagenesis studies then permits the most likely model to be identified from this small pool of structures.

Hydrophobic lining

Although our model of PLN may represent a compact conformation, there is clearly a pore running through the centre of the pentamer. A space-filling representation of slices through the molecule reveals a continuous

a *b*

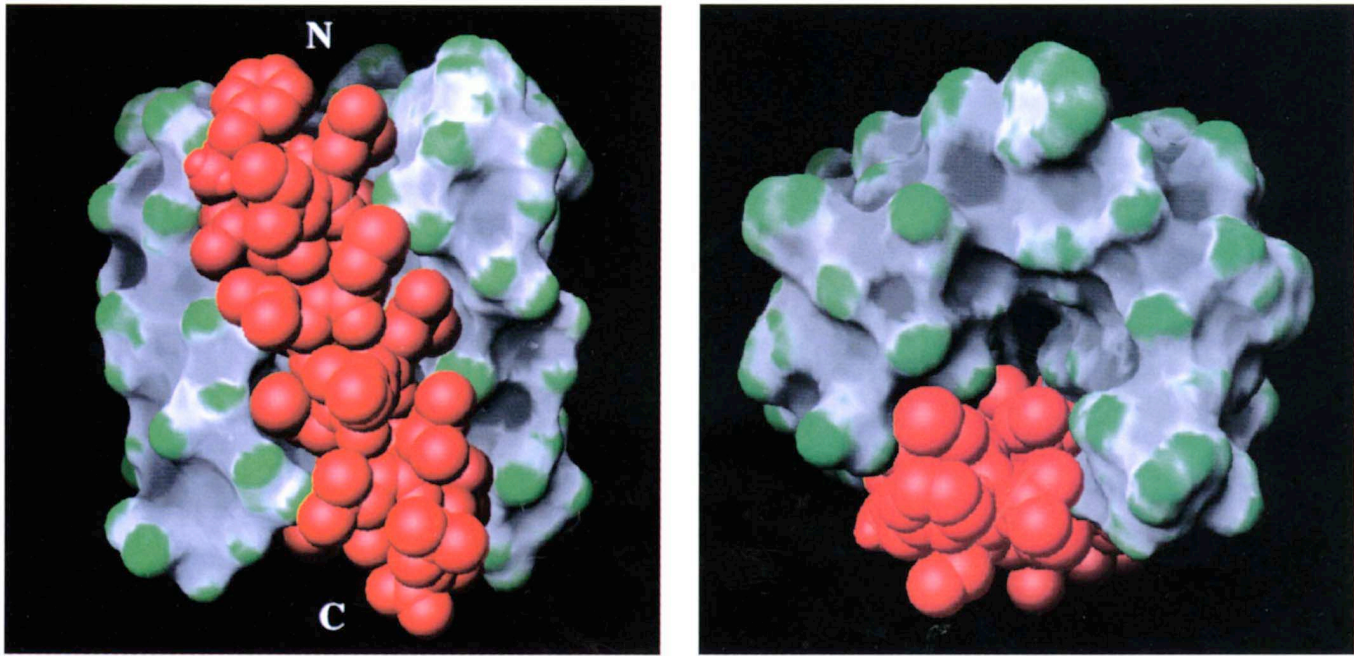

Fig. 5 *a*, The packing interactions between the helices in the phospholamban pentamer. A space-filling representation is used for one helix (red), while a molecular surface coloured by surface curvature[28] is used for the remaining four helices (exposed regions are shaded green, while buried regions are shaded dark grey). *b*, Space-filling representation rotated by 90°, looking along the pore from the N terminus.

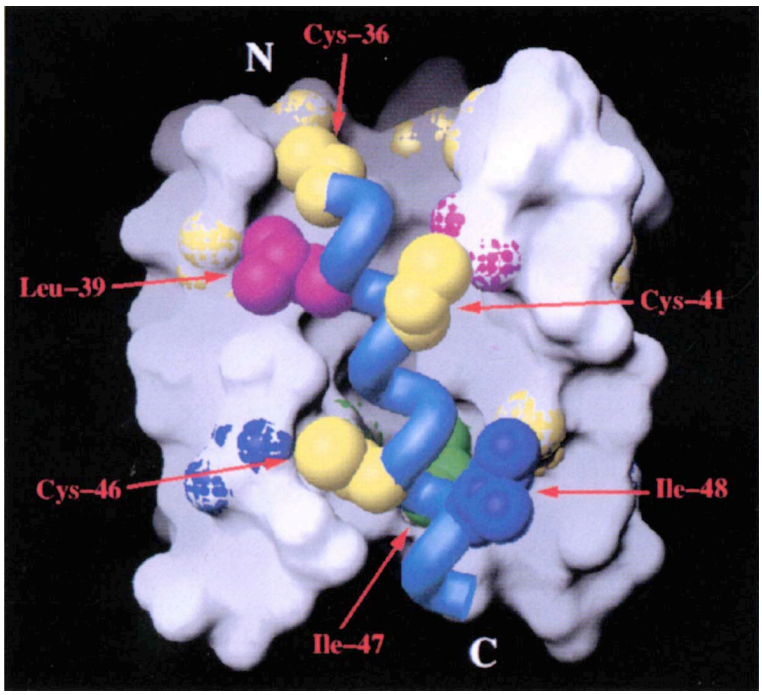

Fig. 6 Location of the three cysteine residues in the phospholamban model. The mainchain of one helix is shown as a thick tube, the other helices are represented by a molecular surface. Cysteine residues are coloured yellow, leucine (residue 39) is coloured magenta, and isoleucine residues are coloured green (residue 47) and blue (residue 48). The same residues on other helices are shown beneath the molecular surface as indicated by the coloured patches.

channel (Fig. 4*b*). The mutationally sensitive residues lie at the interface between adjacent helices, and the most sensitive make contact with the same residue in both adjacent helices. In the case of residues 40, 43 and 47 a three-body interaction is seen with interactions between a helix and its two neighbouring helices. These residues define the narrowest part of the channel which is approximately 3 Å in diameter (Fig. 4*c*).

The helices exhibit a high degree of spatial complementarity at their packing interface (Fig. 5*a,b*). This contributes both to the stability of the pentamer and also provides specificity of interaction. Of considerable interest is the location of the cysteine residues in the structure. These represent the only moderately polar residues in the transmembrane sequence modelled, and therefore might be expected to play some part in the ion channel activity of the pentamer. Cys 36 is at the entrance to the pore formed by the pentamer, and therefore is in a position to influence the ion channel activity of phospholamban (Fig. 6). We speculate that Cys 36 is the site of Cd^{2+} inactivation of the channel, based on its accessibility and its pore location. In contrast, both Cys 41 and 46 are located partially on the external (lipid facing) face of the pentamer. Both these residues are involved in the packing interface between adjacent helices. Cys 41 packs against Leu 39 on the neighbouring helix, while Cys 46 interacts with both Iso 47 and 48. It is possible that all the cysteine residues play some role in defining the overall electrostatic properties of the phospholamban pore; however, only Cys 36 is placed so as to make a direct interaction with ions.

The putative PLN pore is predominately (apart from Cys 36) lined by hydrophobic residues (Figs. 4*b*, 7). That an ion channel may possess a hydrophobic lining has been suggested previously[15] and is supported by experimental work[20]. This is in contrast to current theories about the residues lining the pores of larger ion channels where polar residues are thought to play a significant role[21–23]. That PLN possesses ion channel activity *in vitro* has been demonstrated[4,5]. The sequence of the PLN transmembrane region dictates that a pore lined with predominantly hydrophobic residues be formed (Fig. 1*b*); if it is assumed that the channel pore is filled with water molecules, the unfavourable ion desolvation energy could be partially compensated for by interaction with the water molecules within the pore. The model presented here for phospholamban, combined with experimental data, provides a starting point for understanding the properties of a hydrophobic pore.

Methods

Mutagenesis. The full details of mutagenesis experiments are presented elsewhere[12]. Briefly, standard molecular biology techniques were used to construct chimeras of full length PLN linked, by a flexible region, to the protein staphylococcal nuclease. Each residue within the transmembrane region was then separately altered by saturation mutagenesis. The ability of each mutant to form pentameric complexes in SDS-PAGE was then determined. The effect of each mutation on pentameric stability was assessed as non-disruptive, partially disruptive, or totally disruptive. A value between 0 and 1 was assigned to each residue examined in the mutation study, reflecting the extent to which mutations at this position disrupted pentamerization. This index was a real number defined by the sensitivity of each residue (*i*) to mutation. The index was normalized to the number of possible observable mutations (N, N=10 in this study). For the n_i observed mutations for a given residue, the effect was quantified (s) using a three point scale. A completely disruptive mutation was assigned a value of 10, partially disruptive mutations a value of 5, and non-disruptive mutations a value of 0. The index (P) was calculated using $P_i = (N/n_i)\ \Sigma^{ni}_{k=1}\ s_{in}$

Molecular dynamics calculations. All calculations were carried out using the program X-PLOR (ref. 24). The united atom topology and parameters sets TOPH19 and PARAM19 (ref. 25) were used with all polar hydrogens included. A nonbonded cutoff of 13 Å was used for all calculations. A switching function was applied to the van der Waals' terms between 10 Å and 12 Å, and a shifting function was applied to the electrostatic term between 10 Å and 12 Å. The bond lengths for hydrogen atoms were constrained to ideal lengths using the SHAKE algorithm[26]. Half-sided distance restraints were applied between O_i and N_{i+4} in order to maintain an α-helical conformation during the systematic search procedure. Distance restraints, using a square-well potential, were applied in order to prevent the separation of helices during simulated annealing[17]. Different restraints were used for two-body and pentamer searches; the details of which are outlined for each case below. All calculations were carried out *in vacuo*, thus speeding convergence. The initial coordinates were those of a canonical α-helix (3.6 residues per turn) derived from internal coordinates. In contrast to (ref. 10), no prior supercoiling was applied to α-helices. Helices were allowed to reach a stable coiled-coil conformation during the annealing procedure. In both two-body and pentamer searches the same simulated annealing schedule was used in order to search the energy surface of the system for local minima. Bad steric contacts present in the initial models were removed by energy minimization with a quartic

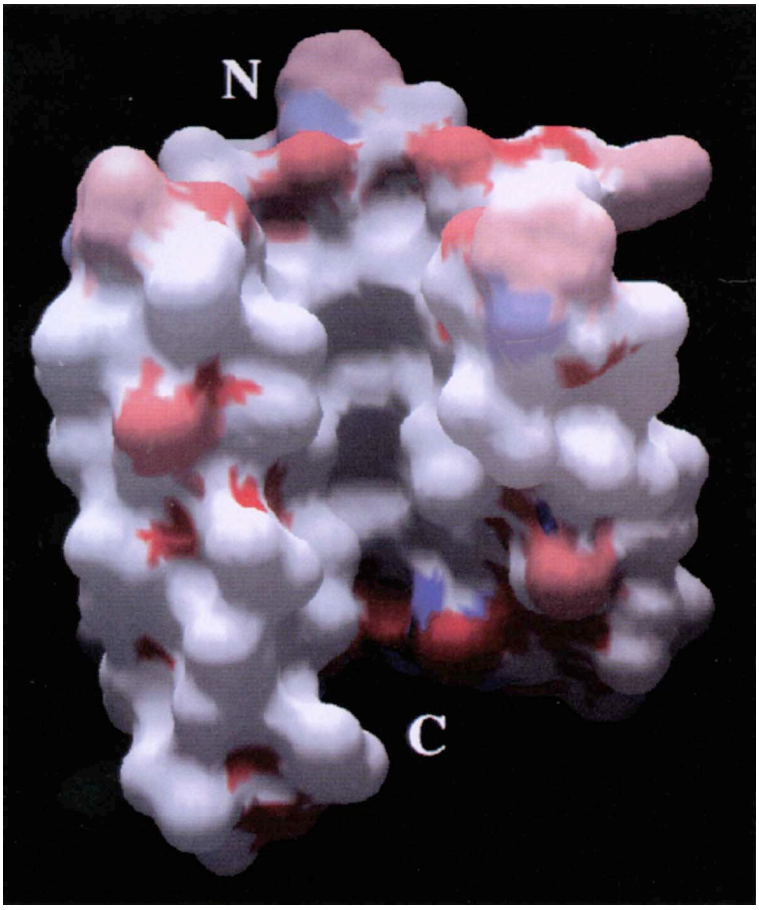

Fig. 7 Partial atomic charges (as defined in the TOPH19 united atom topology set[25]) projected onto the molecular surface for four of the five α-helices of phospholamban (the fifth helix is removed to illustrate the continuous channel that is present through the centre of the pentamer). Negative charge is coloured red while positive charge is blue, white indicates zero partial charge.

repulsive function instead of the usual van der Waals' and Coulombic terms. This was followed by energy minimization using the standard nonbonded potential. The atoms were then assigned random velocities from a Maxwell distribution. The system was simulated using molecular dynamics for 5,000 steps at 600 K with a timestep of 1 fs. This was followed by simulation, 5,000 steps, at the lower temperature of 300 K with a timestep of 2 fs. Constant temperature was maintained by coupling to a heat bath[27]. The molecular dynamics simulation was followed by energy minimization.

The two-body search. An exhaustive search of the possible interactions between the parallel helices was carried out. Changes were made to previous work[10] to improve both the range and evenness of sampling. The search was carried out over the entire two-body rotational interaction space (α = 0°–360°, β = 0°–360°, where α and β are the rotation angles about the long axis of the two helices relative to some arbitary starting position). Tests showed that initial crossing angles (Ω) between +20° and -20° often became trapped in local minima around 0°, therefore, the starting structures were canonical α-helices with either a left-handed +50° or right-handed -50° crossing angle. These initial crossing angles allow convergence to stable left-handed and right-handed coiled-coil structures, including configurations close to Ω=0° (for example Fig. 2*d*, structures d5 and d6). Multiple trials were carried out from the same starting position, using different initial random velocities in each case. The centres of the helices were initially separated by 10.4 Å , with the maximum centre-centre distance restrained to 10.4 Å with a half-sided potential.

Averaging of structures from the two-body search. A convention was used in order to localize different structures to unique regions of rotational space. The dyad axis of each final structure was aligned along the *z*-axis in coordinate space and the geometric centres of both helices were calculated. The *z* components of the centres were compared and the helix with the more positive value was assigned the identifier A, the other assigned the identifier B. Therefore, helix A always has a positive or zero shift, along the long helix axis, with respect to helix B. When considering plots of rotation angles α against β it must be remembered that points on either side of the dyad axis are not equivalent because of this convention. Clusters of structures were determined visually from plots of α against β, (Fig. 2c; in general clusters were well defined). The average structure for each cluster was then energy minimized using a repulsive nonbonded potential in order to regularize any bad contacts and distorted side-chain geometries. This regularized structure was then subjected to the same simulated annealing protocol used in the systematic search.

Generation of pentamers from dimers. Analysis of the final helical pair conformations was carried out to identify interactions between pairs that were consistent with a pentamer. The rotation matrix (σ) and translation vector (τ) required to superimpose the Cα atoms of helix A on helix B was calculated. This transformation was then repeatedly applied to the coordinates ($\vec{r}_1$) of helix A to generate a structure with five helices (helix B was first deleted), $\vec{r}_{i+1} = \sigma\vec{r}_i + T$. The r.m.s. difference between the α-coordinates of the first helix and a sixth helix generated by rotation and translation of the fifth helix was calculated. This residual (*R*) was used as a measure of the lack of closure of the pentamer generated (ideally the sixth helix should superimpose on the first),

$$R = \text{sqrt}\,(\Sigma\,(\vec{r}_1 - \vec{r}_6)^2 / N_{C\alpha}) \qquad (1)$$

where the sum is over all Cα coordinates and $N_{C\alpha}$ is the number of Cα atoms in the monomer.

The symmetric pentamer search. Initial symmetric, pentameric structures were generated from canonical α-helices. The initial helix was defined to be 9.5 Å from the centre of the pentameric axis. The helix was then duplicated and rotated by 72° around this axis. This duplication was repeated four times to generate the pentamer. An initial crossing angle was imposed by rotation of the long helix axis with respect to the pentamer long axis. The crossing angle was 15° for the initial left-handed model and -30° for the initial right-handed model. The distance between the centres of neighbouring helices was restrained to a maximum distance of 11 Å using a half-sided potential. No restraint was applied between the helices and the pentamer axis. The search was with respect to only one variable, the rotation about the long axis of each helix. A symmetric pentamer was assumed, thus allowing a rotation to be applied to all helices simultaneously. The search was across the whole rotation space (α = 0°–360°) in 20° steps, simulated annealing was performed to relax the conformation without explicit application of symmetry restraints. In addition, multiple trials were carried out from the same starting position, using different initial random velocities in each case.

Measuring the degree of pentameric symmetry. The residual *R* (equation 1) cannot be used to assess the lack of closure of pre-formed pentamers not derived by repeated transformation of one helix. Therefore, a criterion was defined to distinguish regular symmetric pentamers from distorted assemblies of five helices: the fit of the five helices to a cylinder with axis $\vec{r}_0$ and radius c,

$$\vec{r}_0 = \frac{\sum_{n=1}^{5} \vec{r}_n}{5} \qquad (2)$$

$$c = \frac{\sum_{n=1}^{5} |\vec{r}_n - \vec{r}_0|}{5} \qquad (3)$$

The r.m.s. deviation of the position of both ends and the centre (defined by the geometric average of Cα coordinates) of each helix from this cylinder was calculated by,

$$P_{r.m.s.d.} = \text{sqrt}\left(\frac{\sum_{n=1}^{5} |\vec{r}_n - \vec{r}_t|-c^2}{5}\right) \quad (4)$$

Visual inspection of structures showed that an r.m.s. deviation greater than 1.5 Å clearly indicated a non-symmetric and non-pentameric arrangement of helices.

Averaging of structures from the pentamer search. Averaging of the pentamer structures could not use the same convention used for pairs of helices. Averaging considered all models within a region of rotation space (α - width ≤ α ≤ α + width), the centre of the averaging region was determined by visual inspection of clusters and the width was 15°. A restriction was applied such that only pentameric structures were considered in the averaging process. This was done by only accepting structures with a value of $P_{r.m.s.d.}$ less than or equal to 1.5 Å. Geometric averages of coordinates were calculated if at least five structures were found. Minimization and simulated annealing were carried out as for the two-body averaging procedure.

Calculation of the interaction energy per residue. The average interaction energy per residue for pentamers was calculated in order to determine the contribution each residue makes to pentamer stability. The nonbonded interaction energy was calculated between residue *i* on helix *n* and all other residues *j* on all other helices *m* (excluding helix *n*),

$$E_{inter} = \sum_{n}\sum_{i} \left(\sum_{m,m\neq n}\sum_{j} E^{vdw}(i_n j_m + E^{elec}(i_n j_m)\right) \quad (5)$$

where $E^{vdw}(i_n j_m$ and $E^{elec}(i_n j_m)$ denotes all van der Waals' and electrostatic energy terms between the residues i_n and j_m.

Calculation of the pore radius. Sections of 2.5 Å thickness were taken along the length of the pentamer at 1 Å intervals. In each section the atoms (one from each helix) closest to the centre of the pore were identified. The geometric centre of these five atoms was calculated and the distance from this centre, in the plane perpendicular to the pore axis, calculated for each of the atoms. We defined the pore radius as the average of these distances minus the corresponding atomic van der Waals' radii. We used the average radius as opposed to the minimum radius in order to take into account flexibility of side chains.

Received 21 October; accepted 14 December 1994.

Acknowledgements
We thank M.Lemmon, L. Rice and W. DeLano for critical readings of the manuscript. This work was supported by grants from the National Institutes of Health, National Science Foundation, funds from Boehringer Ingelheim Inc. and the National Foundation for Cancer Research to D.M.E; and by a grant from the National Science Foundation AC S 93-181159 to A.T.B. The coordinates of the phospholamban model will be deposited in the Brookhaven Protein Data Bank.

1. Kirchberger, M.A., Tada, M. & Katz, A.M. Phospholamban: a regulatory protein of the cardiac sarcoplasmic reticulum. *Recent Advances in Studies on Cardiac Structure and Metabolism* **5**, 103–115 (1975).
2. James, P., Inui, M., Tada, M., Chiesi, M. & Carafoli, E. Nature and site of phospholamban regulation of the Ca^{2+} pump of sarcoplasmic reticulum. *Nature* **342**, 90–92 (1989).
3. Simmerman, H.K.B., Lovelace, D.E. & Jones, L.R. Secondary structure of detergent solubilized phospholamban, a phophorylatable, oligomeric protein of cardiac sarcoplasmic reticulum. *Biochim. biophys. Acta* **997**, 322–329 (1989).
4. Kovacs, R.J., Nelson, M.T., Simmerman, H.K.B. & Jones, L.R. Phospholamban forms Ca^{2+}-selective channels in lipid bilayers. *J. biol. Chem.* **263**, 18364–18368 (1988).
5. Arkin, I.T., Moczydlowski, E.G., Aimoto, S., Smith, S.O. & Engelman, D.M. Functional and structural studies of phospholamban as a model ion channel protein. *Biophys. J.* **64**, A207 (1993).
6. Wallace, B.A. & Ravikumar, K. The gramicidin pore: crystal structure of the caesium complex. *Science* **241**, 182–187 (1988).
7. Fox, R.O. & Richards, F.M. A voltage-gated ion channel model inferred from the crystal structure of alamethicin at 1.5 Å resolution. *Nature* **300**, 325–330 (1982).
8. Cascio, M. & Wallace, B.A. Conformation of alamethicin in phospholipid vesicles, implications for insertion models. *Proteins* **4**, 89–98 (1988).
9. Unwin, N. Nicotinic acetylcholine receptor at 9 Å resolution. *J. molec. Biol.* **229**, 1101-1124 (1993).
10. Treutlein, H.R., Lemmon, M.A., Engelman, D.M. & Brünger, A.T. The glycophorin A transmembrane domain dimer: Sequence-specific propensity for a right-handed supercoil of helices. *Biochemistry* **31**, 12726–12733 (1992).
11. Lemmon, M.A., Treutlein, H.R., Adams, P.D., Brünger, A.T. & Engelman, D.M. A dimerization motif for transmembrane α-helices. *Nature struct. Biol.* **1**, 157–163 (1994).
12. Arkin, I.T., Adams, P.D., MacKenzie, K.R., Lemmon, M.A., Brünger, A.T. & Engelman, D.M. Structural organization of the pentameric transmembrane α-helices of phospholamban, a cardiac ion channel. *EMBO J.* **13**, 4757–4764 (1994).
13. Lemmon, M.A. & Engelman, D.M. Specificity and promiscuity in membrane helix interactions. *Q. Rev. Biophys.* **27**, 157–218 (1994).
14. Lemmon, M.A., Flanagan, J.M., Treutlein, H.R., Zhang, J. & Engelman, D.M. Sequence-specific dimerization of transmembrane α-helices. *Biochemistry* **31**, 12719–12725 (1992).
15. Popot, J.L. & Engelman, D.M. Membrane protein folding and oligomerization: the two-stage model. *Biochemistry* **29**, 4031–4037 (1990).
16. Novotny, J., Rashin, A.A. & Bruccoleri, R.E. Criteria that discriminate between native proteins and incorrectly folded models. *Proteins* **4**, 19–30 (1988).
17. Nilges, M. & Brünger, A.T. Automated modeling of coiled coils: Application to the GCN4 dimerization region. *Prot. Engng.* **4**, 649 (1991).
18. DeLano, W. & Brünger, A.T. Helix packing in proteins: prediction and energetic analysis of dimeric, trimeric, and tetrameric GCN4 coiled coil structures. *Proteins* **20**, 105–124 (1994).
19. Kerr, I.D., Sankararamakrishnan, R., Smart, O.S., & Sansom, M.S.P. Parallel helix bundles and ion channels: Molecular modeling via simulated annealing and restrained molecular dynamics. *Biophys. J.* **67**, 1501–1515 (1994).
20. Menestrina, G., Voges, K-P., Jung, G., & Boheim, G. Voltage-dependent channel formation by rods of helical polypeptides. *J. membrane Biol* **93**, 111–132 (1986).
21. Lear, J.D., Wasserman, Z.R. & DeGrado, W.F. Synthetic amphiphilic peptide models for protein ion channels. *Science* **240**, 1177–1181 (1988).
22. Bertrand, D., Galzi, J.L., Devillers-Thiéry, A., Bertrand, S. & Changeux, J.P. Stratification of the channel domain in neurotransmitter receptors. *Curr. Opin. Cell Biol.* **5** 688–693 (1993).
23. Xu, M. & Akabas, M.H. Amino acids lining the channel of the g-aminobutyric acid type A receptor identified by cysteine substitution. *J. biol. Chem.* **268**, 21505–21508 (1993).
24. Brünger, A.T. *X-PLOR Version 3.1* (Yale University, New Haven, CT, 1992).
25. Brooks, B.R., Bruccoleri, R.E., Olafson, B.D., States, D.J., Swaminathan, S. & Karplus, M. CHARMM: A program for macromolecular energy, minimization, and dynamics calculations. *J. comp. Chem.* **4**, 187 (1983).
26. Ryckaert, J.P., Ciccotti, G. & Berendsen, H.J.C. Numerical integration of the Cartesian equations of motion of a system with constraints: Molecular dynamics of *n*-alkanes. *J. comp. Phys.* **23**, 327–341 (1977).
27. Berendsen, H.J.C., Postma, J.P.M., van Gunsteren, W.F., DiNola, A. & Haak, J.R. Molecular dynamics with coupling to an external bath. *J. Chem. Phys* 81, 3684–3690 (1984).
28. Nicholls, A. & Honig B. *GRASP Manual.* (Columbia University, New York, NY, 1992).